The Two-Dimensional S = 1 Quantum Heisenberg Antiferromagnet at Finite Temperatures

Kenji Harada, Matthias Troyer¹ and Naoki Kawashima²

Division of Applied Systems Science, Kyoto University, Sakyo-ku, Kyoto 606-01

Institute for Solid State Physics, University of Tokyo, Roppongi 7-22-1, Tokyo 106

Department of Physics, Toho University, Miyama 2-2-1, Funabashi 274, Japan

(Received December 2, 2024)

The temperature dependence of the correlation length, susceptibilities and the magnetic structure factor of the two-dimensional spin-1 square lattice quantum Heisenberg antiferromagnet is computed by the quantum Monte Carlo loop algorithm (QMC). In the experimentally relevant temperature regime the theoretically predicted asymptotic low temperature behavior is found to be not valid. The QMC results though agree reasonably well with experimental results on La_2NiO_4 even without considering anisotropies in the exchange interactions.

KEYWORDS: Heisenberg model, quantum Monte Carlo

Recently, field theoretical predictions^{1,2,3)} concerning the correlation length of the square lattice quantum Heisenberg antiferromagnet(QHA) were directly checked by experimental measurements^{4,5)} and several quantum Monte Carlo (QMC) simulations.^{6,7,8,9)} While in the case of spin S=1/2 the validity of the predictions seemed supported by experiments, in the case of S=1, experimental measurements in both La₂NiO₄⁴⁾ and K₂NiF₄⁵⁾ turned out to be inconsistent with the theoretical predictions.

The inconsistencies were explained by noting that the theoretical low temperature expression are valid at the temperatures of the S=1/2 experiments but not valid in the temperature regime of the S=1 experiments. While a number of simulations have been performed for S=1/2, only a high temperature series expansion calculation¹⁰⁾ and an effective high temperature theory (PQSCHA)¹¹⁾ are available for S=1 in the experimentally relevant temperature range. In this paper we compute the correlation length and other thermal averages for the S=1 QHA on a square lattice by the quantum Monte Carlo loop algorithm¹²⁾ generalized to larger spins. ^{13, 14)} It was implemented in continuous imaginary-time representation¹⁵⁾ to eliminate the systematic error due to Suzuki-Trotter discretization of path integrals.

When implemented in continuous imaginary time, the probability for the graph assignment in the cluster algorithms for larger spins become much simpler than the original discrete time version¹³⁾ although the idea is essentially the same. As in the case of discrete time, we first extend the Hilbert space by expressing each spin operator by a sum of 2S Pauli spins:

$$S_i = \frac{1}{2} \sum_{\mu=1}^{2S} \sigma_{i\mu}.$$
 (1)

We therefore consider (2SN) vertical lines along the imaginary time axis, each specified by two indices $(i\mu)$, where N is the total number of original spins. Since there

are unphysical states in the new Hilbert space, in which some of spins have magnitude less than S, we have to eliminate such states by applying projection operators. We here use a representation where z-spin components are diagonalized. Our procedure for the graph assignment is that, for each pair of neighboring world lines and for each uninterrupted time interval during which spins on these world lines are antiparallel, we generate "cuts" of worldlines with probability density J/2. At each cut, we reconnect pairwise the four end points created by the cut by two horizontal segments (Fig.1). The application of the above-mentioned projection operator for a site is realized by choosing an appropriate boundary condition in the temporal direction. If the spin values $(\sigma_{(iu)}^z(\tau))$ are the same at the four end points, (i1) and (i2) at $\tau = \beta$ and those at $\tau = 0$, we choose straight connection (connecting (i1) at $\tau = \beta$ to (i1) at $\tau = 0$) and cross connection (connecting (i1) at $\tau = \beta$ to (i2) at $\tau = 0$) with equal probability. Otherwise, we choose the unique way for connecting these four points pairwise so that the spin value at each connection point is continuous. Thus we form many loops which are to be flipped with probability 1/2. This algorithm turns out to be quite efficient as its discrete version.

Using chiral perturbation theory, Hasenfratz and Niedermayer $(HN)^2$ obtained the temperature dependence of the correlation length up to two-loop order for an arbitrary magnitude of spin:

$$\xi_{HN} = \frac{e}{8} \frac{\hbar c}{2\pi \rho_s} \exp\left(\frac{1}{t}\right) \times \left[1 - \frac{t}{2} + \mathcal{O}\left(t^2\right)\right], \quad (2)$$

where $t \equiv k_{\rm B}T/2\pi\rho_S$. The dependence on the magnitude of the spin S is only implicit through the S-dependence of the the spin-stiffness constant ρ_s , and the spin wave velocity c. For S = 1/2 the spin wave theory (SWT)¹⁶⁾ values for ρ_s and c were found to be close to the QMC estimates. As SWT is better for larger spins we can confidently use the SWT values for S = 1 in the following:

 $2\pi\rho_s = 5.461J$ and $\hbar c = 3.067J$. These values should be within 1% relative errors from the exact ones.

Equation (2) is valid in the renormalized classical regime where

$$t \ll 1$$
, and $t \ll \frac{\hbar c}{2\pi\rho_s} \approx \frac{\sqrt{2}}{\pi} \frac{1}{S} \left(1 + \frac{0.196}{S} \right)$. (3)

The approximation in the last term on the right hand side is again the leading order SWT result.

In the case of S=1/2 QHA it was found by QMC simulations that Eq. (2) is valid only at very large correlation lengths,^{8,9)} of the order of 100 lattice spacings or larger. In the experimentally relevant temperature regime the deviations, while clearly visible in the QMC simulations, are however smaller than the experimental errors. Thus the theory and experiment agree for S=1/2.

The observed large discrepancies for $S=1^{4,5}$ are somewhat counter-intuitive, since the theory based on a spin-wave picture should be better for larger spins. Actually however, as noted before in Refs. 1,8,9,10, it can be seen from Eq. (3) that the temperature regime where the asymptotic expression is valid is lower for larger S. There is a simple explanation. Larger spins are more classical and thus the quantum effects, which determine Eq. (2) are cut off at lower temperatures for larger spins. The validity of Eq. (2) is then restricted to even larger correlation lengths than for S=1/2, much larger than accessible in experiments.

As the analytic low temperature form is not valid in the experimentally accessible temperature regime, we performed QMC simulations over the temperature range $t \geq 0.18$ ($k_{\rm B}T \geq J$) to compare the experimental data⁴) with the S=1 QHA. The second moment correlation length ξ_L on a finite system of size L was determined from the static structure factor $S_L(\mathbf{q})$ in the vicinity of $\mathbf{Q} = (\pi, \pi)$.¹⁷ The ξ_L is calculated as follows:

$$\xi_L^{-2} \equiv f(2\pi/L, 0) + f(0, 2\pi/L) - f(2\pi/L, 2\pi/L), \quad (4)$$

where

$$f(\mathbf{q}) \equiv 4\sin^2\left(\frac{\mathbf{q}}{2}\right) \left(1 - \frac{S(\mathbf{Q} + \mathbf{q})}{S(\mathbf{Q})}\right)^{-1},$$
 (5)

This estimator for the correlation length (of a finite system) should be correct up to the fourth order in $2\pi/L$. We use improved estimators to reduce the statical errors. For a given temperature T, when the lattice size L is sufficiently large, the ξ_L converges to a size-independent value $\xi(T)$, which we regard as the infinite-size limit. We find that the convergence is achieved to the accuracy determined by the present statistical error when the condition $L \geq 7\xi_L$ is satisfied. All the following results are obtained under this condition. And for each simulation we have performed 10^6 sweeps, after 10^4 thermalization sweeps.

A selection of our results of the correlation length ξ , the staggered structure factor $S(\pi,\pi)$ and the uniform susceptibility χ are summarized in Tab.I. In Fig.2, we plot our QMC results for the correlation length together with the experimental data,⁴⁾ and theoretical predictions

Eq. (2). Our present estimates are in rough agreement with experimental measurements. Greven *et al.* and Nakajima *et al.* have proposed to additionally include the effects of a small Ising anisotropy using a mean-field type correction to the theoretical isotropic results. This correction (Eq.(7) in Ref. 4) however makes the agreements worse, as can be seen in Fig.2.

Comparing to theoretical predictions we find that the data deviate strongly from the low temperature formula Eq. (2). The effective PQSCHA approximation, ¹¹⁾ an effective high temperature theory however agrees well with the QMC results, much better than for S = 1/2.7,11)

Another violation of the theoretical predictions^{1,3)} was observed in the peak value of the staggered structure factor $S(\pi, \pi)$, which according to the theory^{1,3,18)} should scale as:

$$S(\pi, \pi) = A2\pi M^2 \xi^2 t^2 (1 + Ct). \tag{6}$$

Here M is the staggered magnetization of the ground state and A and C universal constants. For spin-1/2 the leading t^2 form was confirmed by high temperature series.¹⁰⁾ Recent QMC data⁹⁾ at lower temperatures fit the above form very well in the temperature range t < 3 with $A \approx 4.0(1)$ and $C \approx 0.5(1)$. Experiments for both S = 1/2 and S = 1 however were better described by an empirical law^{4,5)}

$$S(\pi,\pi) \propto \xi^2$$
 (7)

over the same temperature range.

We applied χ^2 analysis to check the consistency of the spin-1 data. Good fits were obtained for t < 0.28, with with $\chi^2 \sim 1$ when we allow C to vary, and $\chi^2 \sim 2$ with fixed C = 0.5. The universal constant A was found to be A = 4.1(1) and A = 4.5(1) respectively, similar to the values obtained for S = 1/2. The discrepancies between the fits are non-universal effects caused by the rather high temperatures.

Comparing our data with the experiments in Fig.3, we can see that for low temperatures the experimental data are consistent with the QMC results and Eq. (6). The discrepancies that lead the authors of Refs. 4, 5 to predict Eq. (7) occur at higher temperatures where the experimental data has large error bars. In view of the precision of our QMC results and the large errors of the experimental results we suspect that, contrary to the suggestion of the authors of Refs. 4,5, the deviations from Eq. (6) are due to uncertainties in the experimental measurements.

Finally we present in Fig.4 the uniform susceptibility for S=1/2 together with previously published S=1/2 results. First we note that, as expected, the asymptotic low temperature behavior of the renormalized classical regime

$$\chi = \frac{2\rho_s}{3} \left(\frac{g\mu_B}{\hbar c}\right)^2 (1 + t + t^2) \tag{8}$$

sets in at lower temperatures for S = 1 than for S = 1/2. It was found that for S = 1/2 the uniform susceptibility is the only quantity for which a clear crossover to quantum critical behavior³ can be observed at interme-

quantum critical behavior³⁾ can be observed at intermediate temperatures $t \sim 1/3$. The uniform susceptibility

in the quantum critical regime is

$$\chi = \chi_{\perp} + BT \left(\frac{g\mu_B}{\hbar c}\right)^2, \tag{9}$$

with a universal slope $B \approx 0.26(1)^{.3,19)}$ For S=1 however, as discussed above, non-universal corrections become important already at lower temperatures. No quantum critical behavior was thus expected for S=1. We can see in Fig.4 that the uniform susceptibility for S=1 deviates from its universal quantum critical behavior at intermediate temperatures. Its slope is however still surprisingly close to the quantum critical one, indicating that the non-universal corrections are still not very large for S=1.

In summary, we have simulated the spin S=1 quantum Heisenberg antiferromagnet on a square lattice in the experimentally relevant temperature regime $k_{\rm B}T\sim J$. We find a better agreement between the Heisenberg model and experimental data than is expected from the low temperature theory. However, in view of still existing small discrepancies it may be necessary to perform simulations on a model with small anisotropies in the exchange interactions, and to critically check the data analysis of the experiments.

Acknowledgments

We are grateful to A. Chubukuv, S. Sachdev, S. Chakravarty, Y. Endoh and K. Ueda for helpful discussion. We wish to thank A. Cuccoli, V. Tognetti, R. Vaia, and P. Verrucchi for providing the results of their PQSCHA theory and to K. Nakajima for the experimental data on La₂NiO₄. M.T. acknowledges the Aspen Center for Physics which enabled fruitful discussions that were important for this work. The calculations were performed on the Hitachi SR2201 massively parallel computer at the computer center of the University of Tokyo. N.K.'s work is supported by the Grant-in-aid for science research (No.09740320) from the Ministry of education, science and culture.

- S. Chakravarty, B. I. Halperin, and D. R. Nelson: Phys. Rev. B 39 (1989) 2344.
- [2] P. Hasenfratz and F. Niedermayer: Phys. Lett. B 268 (1991) 231.
- [3] A. V. Chubukov, S. Sachdev, and J. Ye: Phys. Rev. B 49 (1994) 11919.
- [4] K. Nakajima, K. Yamada, S. Hosoya, Y. Endoh, M. Greven and R.J. Birgeneau: Z. Phys. B 96 (1995) 479.
- [5] M. Greven, R. J. Birgeneau, Y. Endoh, M. A. Kastner, M. Matsuda and G. Shirane: Z. Phys. B 96 (1995) 465.
- [6] M. S. Makivic and H.-Q. Ding: Phys. Rev. B 43 (1991) 3562.
- [7] J.-K. Kim, D.P. Landau and M. Troyer: Phys. Rev. Lett. 79 (1997) 1583.
- [8] B.B. Beard, R. J. Birgeneau, M. Greven, and U.-J. Wiese: preprint, cond-mat/9709110.
- [9] J.-K. Kim and M. Troyer: preprint cond-mat/9709333.
- [10] N. Elstner et al: Phys. Rev. Lett. 75 (1995) 938.
- [11] A. Cuccoli, V. Tognetti, R. Vaia, and P. Verrucchi: Phys. Rev. Lett. 77 (1996) 3439; Phys. Rev. Lett. 79 (1997) 1584; Phys. Rev. B 56 (1997) 14456.
- [12] H. G. Evertz, M. Marcu, and G. Lana: Phys. Rev. Lett. 70 (1993) 875.
- [13] N. Kawashima: J. Stat. Phys. 82 (1996) 131. N. Kawashima and J.E. Gubernatis: J. Stat. Phys. 80 (1995) 169;

- [14] N. Kawashima and J.E. Gubernatis: Phys. Rev. Lett. 73 (1994) 1295.
- [15] B.B. Beard and U.J. Wiese: Phys. Rev. Lett. 77 (1996) 5130.
- [16] C.J. Hammer, Z. Weihong and J. Oitmaa: Phys. Rev. B 50 (1994) 6877.
- [17] G.A. Baker, Jr and N.Kawashima: Phys. Rev. Lett. 75 (1995) 994.
- [18] A. Chubukov: private communications.
- [19] M. Troyer, M. Imada and K. Ueda: J. Phys. Soc. Jpn. 66 (1997) 2957; M. Troyer and M. Imada in Computer Simulations in Condensed Matter Physics X, ed. D.P. Landau et al., (Springer Verlag, Heidelberg, 1997).

Table I. Correlation length ξ and magnetic structure factor $S(\pi,\pi)$ and uniform susceptibility χ as a function of temperature $t=k_{\rm B}T/2\pi\rho_s$.

$J/k_{\mathrm{B}}T$	t	L	ξ	$S(\pi,\pi)$	χ
0.10	1.83	20	0.298(5)	0.8915(1)	0.051579(6)
0.15	1.22	20	0.396(5)	1.0489(2)	0.068503(9)
0.20	0.92	20	0.497(5)	1.2481(3)	0.08118(1)
0.25	0.73	20	0.610(5)	1.5029(5)	0.09038(1)
0.30	0.61	20	0.739(5)	1.8342(7)	0.09687(2)
0.35	0.52	20	0.894(6)	2.272(1)	0.10108(2)
0.40	0.46	20	1.079(6)	2.854(2)	0.10343(2)
0.45	0.41	20	1.307(6)	3.648(2)	0.10435(3)
0.50	0.37	30	1.604(3)	4.776(1)	0.104000(8)
0.55	0.33	30	1.982(8)	6.392(4)	0.10275(2)
0.60	0.31	40	2.482(5)	8.795(2)	0.100756(8)
0.65	0.28	40	3.14(1)	12.46(1)	0.09829(3)
0.70	0.26	50	4.06(1)	18.25(2)	0.09560(2)
0.75	0.24	50	5.30(2)	27.60(3)	0.09275(3)
0.80	0.23	60	7.06(2)	43.30(5)	0.09000(3)
0.85	0.22	80	9.52(3)	70.03(8)	0.08746(3)
0.90	0.20	120	12.98(4)	116.4(1)	0.08516(3)
0.95	0.19	140	17.97(5)	198.8(3)	0.08309(3)
1.00	0.18	200	24.94(7)	344.0(4)	0.08133(2)

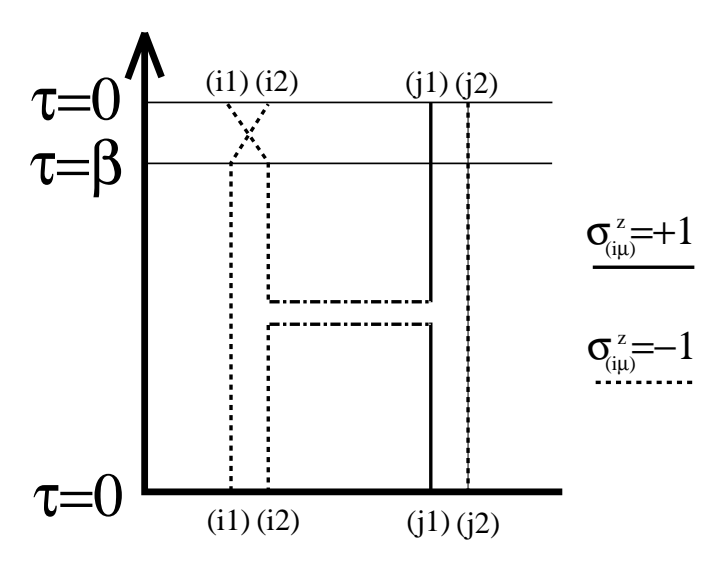


Fig. 1. A cut and two horizontal segments. Two types of boundary condition in temporal direction are also illustrated.

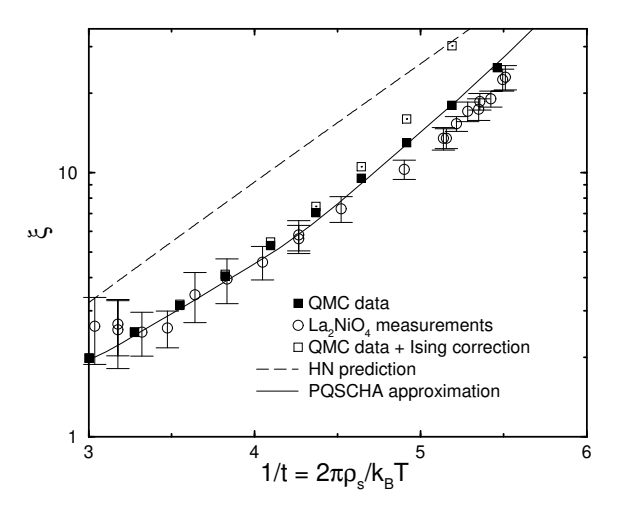
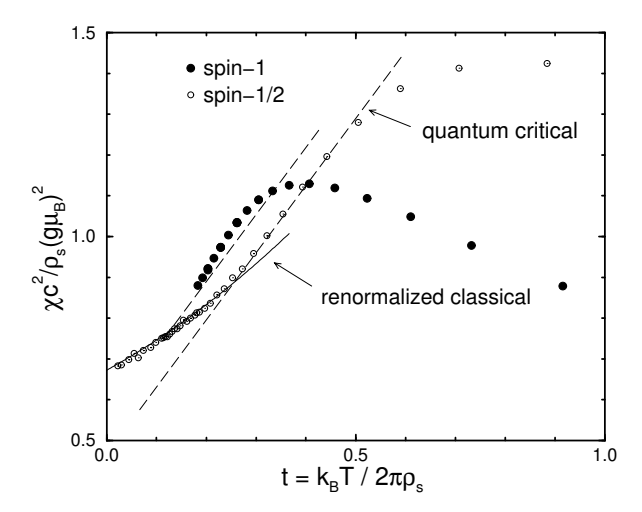


Fig. 2. The correlation length ξ as a function of $t=k_{\rm B}T/2\pi\rho_s$. Filled squares represent the results of our simulation, the open circles are experimental measurements.⁴⁾ While the experimental measurements agree roughly with our QMC results, they are incompatible with the QMC results corrected for a small Ising anisotropy (open squares). Comparing to analytic calculations we find that in this temperature range the low-temperature predictions Eq. (2) (dashed line) is not valid. The PQSCHA approximation¹¹⁾ however agrees well with both our data and the experimental measurements.



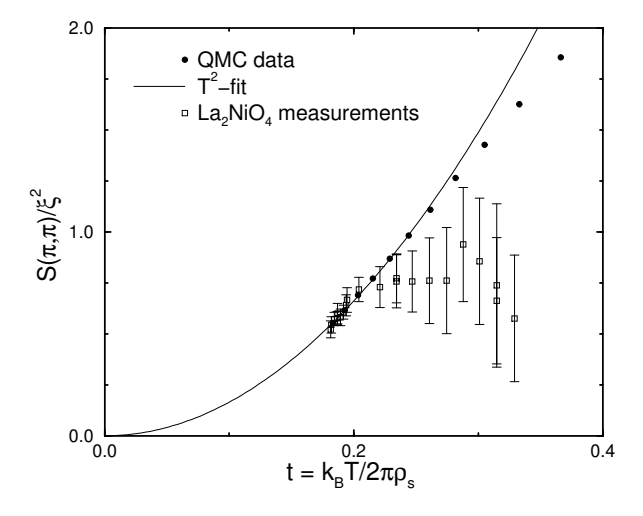


Fig. 3. The ratio of structure factor peak value and square of the correlation length $S(\pi,\pi)/\xi^2$ as a function of temperature. Solid circles are the QMC measurements, open squares the experimental measurements. They agree at low temperatures but differ at higher temperatures. The solid line is a fit of the QMC data to the theoretical low-temperature prediction.

Fig. 4. The uniform susceptibility χ as a function of temperature t for both spin S=1 and spin S=1/2 (taken from Ref. 9). The solid line is the predicted low temperature form of the renormalized classical regime. The dashed lines have the universal slope expected for the quantum critical regime. As expected, contrary to S=1/2 no extended quantum critical regime exists for S=1. However the slope is close to the quantum critical value as non-universal corrections are still small for S=1.